Arabidopsis primary microRNA processing proteins HYL1 and DCL1 define a nuclear body distinct from the Cajal body

Liang Song[†], Meng-Hsuan Han[‡], Joanna Lesicka[§], and Nina Fedoroff[†¶‖]

[†]Biology Department and Huck Institute of the Life Sciences, Pennsylvania State University, University Park, PA 16802; [¶]Santa Fe Institute, Santa Fe, NM 87501; [‡]Department of Biochemistry, Molecular Biology, and Cell Biology, Northwestern University, Evanston, IL 60208-3500; and [§]Department of Gene Expression, Adam Mickiewicz University, Miedzychodzka 5, 60-371 Poznan, Poland

Contributed by Nina Fedoroff, February 5, 2007 (sent for review February 1, 2007)

Small regulatory microRNAs (miRNAs) are encoded in long precursors and are released from them during processing by cleavage within partially duplexed stem–loop structures. In the present work we investigated the role of the *Arabidopsis* nuclear RNA-binding protein HYL1 and the nuclear RNase III enzyme DCL1 in processing of primary miRNA (pri-miR171a). The *miR171a* gene is complex, with multiple transcription start sites, as well as alternative splicing of exons and alternative polyadenylation sites. Both HYL1 and DCL1 proteins are required for processing of the major pri-miR171a, spliced and polyadenylated forms of which accumulate in plants homozygous for mutations in either gene, but not in wild-type plants. In transiently transfected *Arabidopsis* protoplasts, HYL1-mCherry and YFP-DCL1 fusion proteins colocalize to small nuclear bodies similar to Cajal bodies but lacking the Cajal body marker Atcoilin. The HYL1 protein coimmunoprecipitates with miR171a and miR159a precursors, indicating that it is an integral component of the precursor processing machinery. Thus, the distinct HYL1- and DCL1-containing nuclear bodies may be miRNA precursor processing sites. Alternatively, they may be assembly and storage sites for the miRNA precursor processing machinery.

small regulatory RNA | precursor | plant

MicroRNAs (miRNAs) are small regulatory RNAs encoded in the genomes of both plants and animals. The miRNA sequence is embedded within a much larger primary miRNA (pri-miRNA) transcript and cleaved out in two steps. The first cleavage generates a stem–loop intermediate, termed the precursor miRNA (pre-miRNA), and the second cleavage releases the miRNA duplex, one strand of which is used as the regulatory effector (1). Mammals use a single class III RNase III, Dicer, to generate both miRNAs and siRNAs, whereas plants have multiple specialized Dicer-like (DCL) enzymes. Among the four *Arabidopsis* DCLs, DCL1 participates in miRNA biogenesis, whereas the others are involved in various aspects of small RNA-mediated gene silencing (1, 2). In animal cells, pri-miRNAs are processed to pre-miRNAs by the RNase III Drosha in the nucleus, whereas Dicer cleaves the pre-miRNAs in the cytoplasm. Both cleavages are thought to be carried out in the nucleus by DCL1 in *Arabidopsis* (3).

Double-stranded RNA-binding proteins (dsRBPs) participate in both the biogenesis and function of small regulatory RNAs, including miRNA and siRNA. In animals, RNase III family enzymes almost always pair with a dsRBP in miRNA precursor and dsRNA processing and are components of the RNA-induced silencing complex (1). Human DGCR8, known as Pasha in *Caenorhabditis elegans* and *Drosophila*, is the dsRBP partner of Drosha in the nuclear Microprocessor complex that cleaves pri-miRNA to pre-miRNA (4, 5). The *Arabidopsis* HYL1 dsRBP, identified through characterization of an insertion mutant designated *hyponastic leaves 1* (*hyl1*), is required for miRNA biogenesis (6–8). Although little is known about its mechanism of action, it has been reported that HYL1 can bind to DCL1 and is required for precise processing of pri-miRNA (9, 10). However, we have identified an ≈300-kDa protein complex containing HYL1, whereas DCL1 has been reported to be in a much larger complex of >660 kDa (7, 11). We show here that HYL1 and DCL1 participate in the same step in the processing of pri-miRNA171a to pre-miRNA171a and that they are both in small, often perinucleolar bodies distinct from the coilin-containing Cajal bodies that were recently identified as centers for the assembly of protein/siRNA silencing complexes in *Arabidopsis* (12). We further show that miRNA precursors coimmunoprecipitate with HYL1, suggesting that the HYL1- and DCL1-containing bodies are miRNA precursor processing sites. Alternatively, they may represent sites for the assembly and storage of miRNA processing machinery.

Results

HYL1 and DCL1 Are Required for pri-miRNA to pre-miRNA Processing. To gain insight into the role of HYL1 and DCL1 in miRNA biogenesis, we analyzed the relative abundance of precursors of miR171a and miR164b using real-time PCR. Not knowing the structure of either precursor, we used a primer pair that will detect the stem–loop structure corresponding to the predicted pre-miRNA, as well as longer transcripts, and a primer pair that will amplify only pri-miRNA molecules extending beyond the stem–loop, as illustrated in Fig. 1*A*. The abundance of pri-miR171a is >10-fold higher in plants homozygous for either one of two alleles of the *hyl1* mutation, as well as in plants homozygous for the nonlethal weak *dcl1-9* allele. Plants homozygous for the mutant *hen1-1* allele of the *HEN1* gene that encodes an miRNA methyl transferase (13) did not show higher levels of miRNA precursors. We obtained similar results for both miRNA genes tested, as well as with primers capable of detecting both pri-miRNA and pre-miRNA (data not shown).

The observation that both sets of primers gave similar results suggested that the longer precursor accounted for most of the difference in precursor abundance between mutant and wild-type plants. To test this inference directly, we separated small (<200 nt) from large (>200 nt) RNAs by Microcon (Millipore, Billerica, MA) filtration and RT-PCR-amplified the RNA in the filtrate and retentate with primers capable of detecting only the pri-miR171a or both pre- and pri-miR171a. The pri-miRNA primer pair did not amplify fragments from the filtrate, but only from the retentate, indicating that the fractionation was efficient. The primer pair that can detect both pre- and pri-miRNAs amplified sequences approximately equally from the filtrate but showed a difference in abun-

Author contributions: L.S., M.-H.H., J.L., and N.F. designed research; L.S., M.-H.H., and J.L. performed research; L.S. analyzed data; and N.F. wrote the paper.

The authors declare no conflict of interest.

Abbreviations: miRNA, microRNA; pre-miRNA, precursor miRNA; pri-miRNA, primary miRNA; DCL, Dicer-like.

‖To whom correspondence should be addressed. E-mail: nvf1@psu.edu.

This article contains supporting information online at www.pnas.org/cgi/content/full/0701061104/DC1.

CELL BIOLOGY

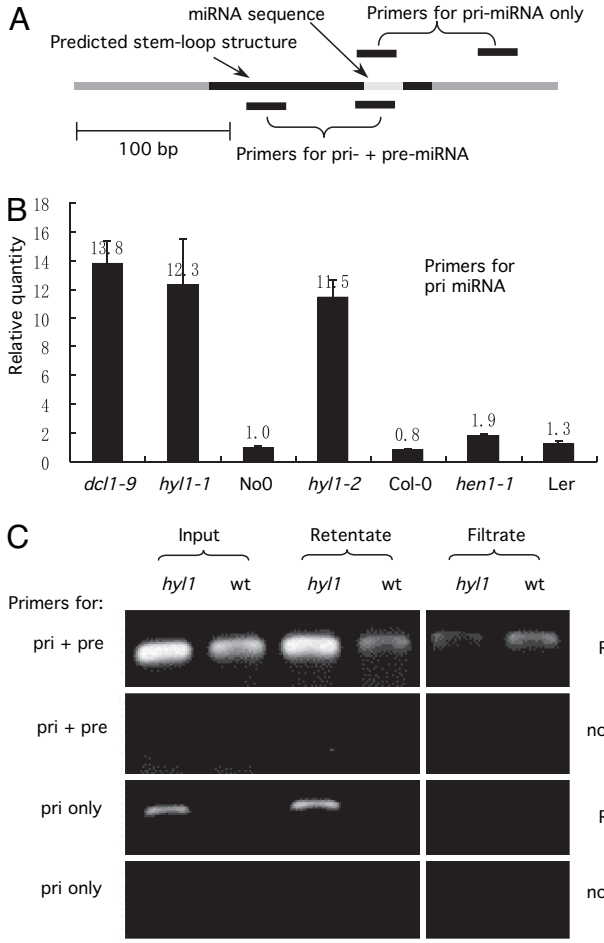

Fig. 1. Pri-miRNA, but not pre-miRNA, is more abundant in *hyl1* and *dcl1* mutants than in wild-type plants. (*A*) A diagrammatic representation of the predicted stem–loop structure containing the mature miRNA sequence encoded by the miR171a gene. (*B*) Real-time PCR amplification of miR171a pri-miRNA from total RNA extracted from 4-week-old plants homozygous for the indicated mutations or wild-type plants of the indicated ecotype. (*C*) RNAs from *hyl1* homozygotes and No-0 wild-type plants were fractionated using a Millipore Microcon filter into molecules shorter than 200 nt (filtrate) and longer than 200 nt (retentate), then amplified by using the primers shown in *A* to detect either both pre-miRNA and pri-miRNAs or just the pri-miRNA.

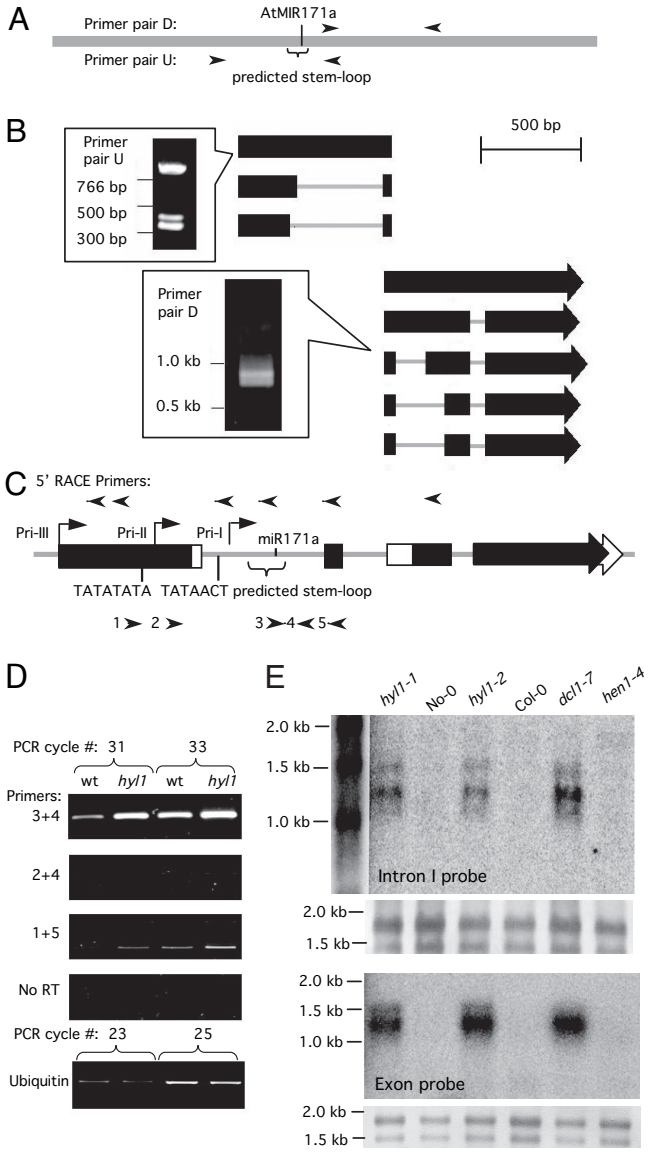

Fig. 2. The structure of the miR171a transcription unit. (*A*) The diagram shows the location of the miR171a, the predicted stem–loop structure containing the pre-miRNA, and the primers used to amplify cDNA fragments from polyA$^+$ RNA. (*B*) Amplified RT-PCR bands and structures deduced from sequencing cloned fragments. (*C*) The structure of the miR171a transcription unit. The black and white arrows represent the alternative forms of exons. Arrowheads above the diagram indicate the nested primers used for 5′ RACE. Right-angled arrows above the diagram show the transcription start sites; the adjacent sequences are those of putative TATA boxes. The arrowheads below the diagram represent the primers used in *D*. (*D*) The relative abundance of different primary transcripts was estimated by semiquantitative RT-PCR. Primers 3 and 4 detect unspliced pri-I, pri-II, and pri-III and spliced pri-I; primers 2 and 4 detect unspliced pri-III and pri-II; primers 1 and 5 detect unspliced and spliced pri-III. (*E*) Northern blots of polyA$^+$ RNA from 4-week-old plants of the indicated genotypes probed with an intron I probe (*Upper*) and an exon probe extending from exon 1 to exon 4 (*Lower*). Loading controls are shown below each blot.

dance in *hyl1* mutant and wild-type plants when used to amplify the large molecules in the retentate, indicating that the difference in abundance was confined to the larger precursor. Amplification was more extensive from the RNA prepared from mutant than wild-type plants, indicating that cleavage of the pri-miR171a to pre-miR171a is reduced in *hyl1* mutant plants, leading to the accumulation of pri-miRNA molecules. The *hyl1* mutation does not completely eliminate precursor processing, and pre-miRNA does not accumulate in the mutant (7).

The miRNA171a Gene Encodes Multiple Transcripts. To understand the structure of the accumulating transcripts, we used the primer pairs U and D (Fig. 2*A*) to amplify sequences upstream and downstream from the putative miRNA171a stem–loop structure. We used polyadenylated RNA because miRNA precursors are often capped and polyadenylated (14, 15). The primer pair U amplified three bands in the 0.3- to 0.9-kb range, and the primer pair D amplified two strong bands and several weaker ones in the 0.9- to 1.1-kb range, each of which was cloned and sequenced (Fig. 2*B*). The upstream fragments correspond to the genomic sequence between the primers (the unspliced transcript) and two alternatively spliced forms that differ in the length of the excised intron. Five different downstream fragments were identified by sequencing and correspond to the unspliced transcript and spliced transcripts from which either one or two introns have been removed. Additional length heterogeneity came from the presence of two alternative polyadenylation sites and the fact that the first two of the three introns had both short and long forms.

We carried out 5′ RACE to identify transcription initiation sites, using the pairs of nested primers shown above the diagram in Fig. 2*C*. Three transcription start sites were identified and designated pri-I, -II, and -III (Fig. 2*C*). The *miR171a* gene has at least three exons, the first of which is identified by the pri-III transcription initiation site. Pri-II is located within the first exon, whereas pri-I is in the first intron 74 bp upstream from the base of the predicted stem–loop structure containing the miR171a sequence. We have also been able to amplify sequences upstream of pri-III by RT-PCR, suggesting that there may either be an additional upstream transcription start site or that there is occasional read-through from an upstream promoter. The overall structure of the *miR171a* transcription unit is quite complex, with multiple transcription start sites, alternative splicing, and alternative polyadenylation sites (Fig. 2*C*). The *miR171a* transcription unit also contains a putative gene encoded entirely within it on the complementary strand. We have detected this transcript, but we find that its abundance is unaffected by the *hyl1* mutation (data not shown).

To assess the relative abundance of the various transcripts, we carried out semiquantitative RT-PCR using the primers shown below the diagram in Fig. 2*C*. Primers 3 and 4, which amplify unspliced pri-I, -II, and -III, as well as spliced pri-I, gave the most intense bands after 31 and 33 cycles of amplification. The other primer pairs, which detect either just pri-III or both pri-III and pri-II, gave much weaker bands even after 33 cycles of amplification. Similar results were obtained with more equally spaced primers (data not shown). These results indicate that the transcription initiation site within the first intron defined by the longer transcripts is used preferentially in both wild-type and *hyl1* mutant plants. Moreover, although it appears that transcripts initiating at both pri-I and pri-III sites are more abundant in *hyl1* mutant than wild-type plants, the bulk of transcripts in both mutant and wild-type plants correspond to transcripts initiated at pri-I. Consistent with the inference that transcripts initiating at pri-I comprise the bulk of the precursor molecules that accumulate in mutant plants, Northern blots probed with either an intron 1 probe or a cDNA probe extending from exon 1 into exon 4 detect the same polyadenylated RNAs, the sizes of which correspond to those expected for unspliced and spliced transcripts initiating at pri-I, predicted to be ≈1.4, 1.1, and 1.0 kb without their polyA tails (Fig. 2*E*). Moreover, the same set of transcripts is detectable in plants homozygous for the *dcl1-7* allele and either allele of the *hyl1* mutation, but not in wild-type plants of either the No-0 or Col-0 ecotype or in *hen1-4* mutant plants (Fig. 2*E*). Thus, mutations in either *hyl1* or *dcl1* result in the accumulation of unspliced and spliced polyadenylated transcripts initiating primarily at pri-I. Although the same transcription start site is preferentially used in wild-type plants (Fig. 2*D*), the transcripts are essentially undetectable by Northern blot analysis (Fig. 2*E*), suggesting that the processing remnants are rapidly degraded when the miRNA processing pathway is intact.

HYL1 and DCL1 Colocalize in Nuclear Bodies. When expressed from a CaMV 35S promoter and transfected into *Arabidopsis* protoplasts, both HYL1-GFP and DCL1-YFP are predominantly in nuclei (Fig. 3). Both proteins are concentrated in one or more small, often perinucleolar bodies in about half of the cells examined and relatively uniformly distributed in the nucleoplasm in the rest. Although recombinant HYL1 and DCL1 can be coimmunoprecipitated (data not shown), as initially reported by Kurihara *et al.* (10), we find them associated with distinct multiprotein complexes of ≈300 kDa and >600 kDa, respectively (7, 11). To determine whether the HYL1 and DCL1 are present in the same nuclear bodies, we made a HYL1-mCherry construct and asked whether it colocalizes with DCL1-YFP in *Arabidopsis* protoplasts. Fig. 4*A* is a positive control that shows colocalization of HYL1-mCherry with HYL1-sGFP. The yellow color of the nuclear foci in the overlaid image indicates that the fluorescence intensity is approximately equal at the detection wavelengths for mCherry (573–628 nm) and GFP (525–550 nm), indicating colocalization of the differently tagged HYL1 proteins. YFP itself accumulates in nuclei (Fig. 4*B*, first and fourth images) but is uniformly distributed in the nucleus and does not show the intense foci characteristic of HYL1-mCherry (Fig. 4*B*, second and fifth images). Moreover, the HYL1-labeled bodies are red in the overlaid image (Fig. 4*B*, third and sixth images), indicating that YFP does not colocalize with HYL1. DCL1-eYFP and HYL1-mCherry colocalize to and within nuclei, often concentrating in perinucleolar bodies, two of which can be seen at different levels in the same cell in Fig. 4*C* (cell C1, layers 1 and 2).

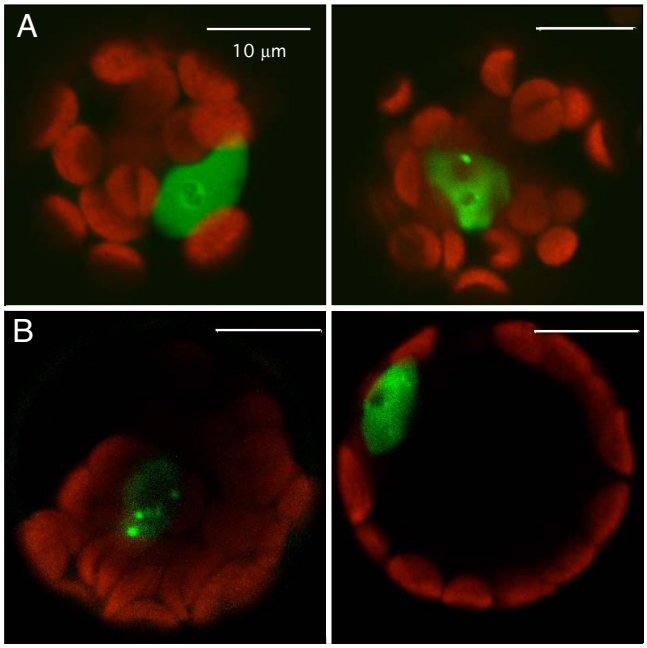

Fig. 3. HYL1 and DCL1 are commonly concentrated in small nuclear bodies. (*A*) Nuclear localization of HYL1-sGFP. (*B*) Nuclear localization of DCL1-eYFP.

Nuclear Bodies Containing HYL1 and DCL1 Are Distinct from Cajal Bodies. The observation that both HYL1 and DCL1 are required for processing pri-miRNA to pre-miRNA *in vivo* and that they often coconcentrate in the same nuclear bodies suggests that these bodies are miRNA precursor processing sites. The miRNA precursor processing complex of animal cells, designated the Microprocessor complex, comprises the RNase III family enzyme Drosha that cleaves the pri-miRNA and an associated RNA-binding protein, DGCR8, that guides the cleavage (4, 5). To determine whether the RNA-binding protein HYL1 physically associates with miRNA precursors, we immunoprecipitated HYL1 from transgenic plants expressing FLAG-tagged HYL1 from a 35S promoter and asked whether miRNA precursors coimmunoprecipitate with it. Precursors for both miR171a and miR159a coimmunoprecipitate with HYL1 after *in vivo* cross-linking of proteins and nucleic acids with formaldehyde (Fig. 5). Thus, HYL1 physically associates with miRNA precursors.

Small perinucleolar bodies, called Cajal bodies, have been described in both plant and animal cells and contain many RNA-processing proteins (14). It was recently reported that *Arabidopsis* Cajal bodies contain some components of the machinery involved in siRNA-mediated silencing and methylation of repetitive DNA (12, 17). Vertebrate Cajal bodies contain a high concentration of coilin, a protein of as yet unknown function that is found uniquely in Cajal bodies, many of whose other proteins are shared with the nucleolus (16). *Arabidopsis* Cajal bodies require a distant homolog of vertebrate coilin, called Atcoilin, for their formation (18). To

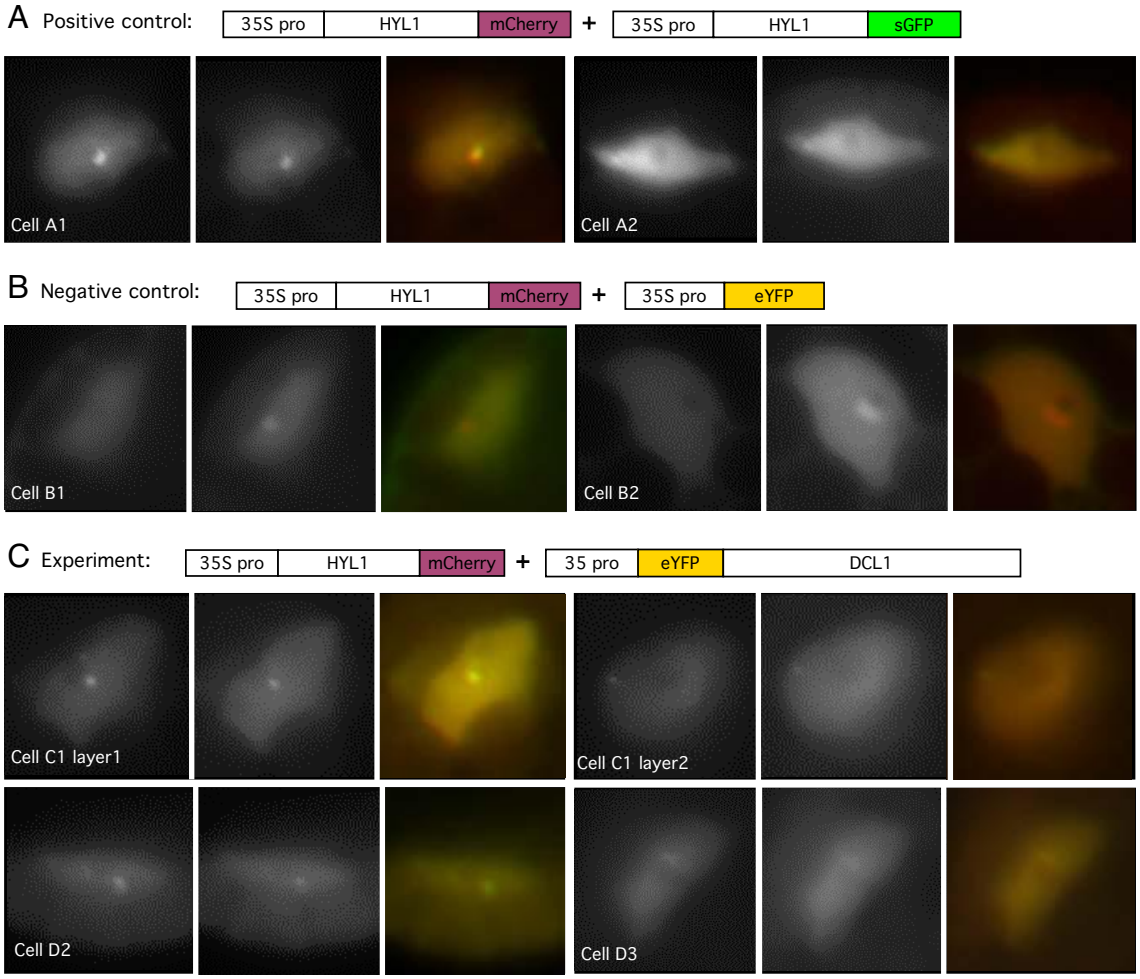

Fig. 4. HYL1 and DCL1 colocalize in nuclear bodies. (*A*) Colocalization of HYL1-mCherry and HYL1-sGFP. (*B*) Coexpressed HYL1-mCherry and eYFP do not colocalize. (*C*) Colocalization of HYL1-mCherry and eYFP-DCL1. (*C Upper*) Two optical sections through the same cell showing colocalization in different bodies in the same nucleus. (*C Lower*) Colocalization of HYL1 and DCL1 in different cells. The green channel (GFP or YFP) is on the left, the red channel (HYL1) is in the middle, and the overlay is on the right for each cell.

determine whether the miRNA precursor-processing proteins HYL1 and DCL1 are also associated with Cajal bodies, we cotransformed *Arabidopsis* protoplasts with 35S-Atcoilin-GFP and 35S-HYL1-mCherry constructs. Both Atcoilin-GFP and HYL1-mCherry localize to small nuclear bodies (Fig. 6), which can be perinucleolar (Fig. 6*B*). However, the two proteins do not colocalize, indicating that the HYL1 and DCL1 proteins define a nuclear body distinct from the Cajal body.

Discussion

In animal cells, pri-miRNA is cleaved to pre-miRNA by the nuclear Microprocessor complex comprising the RNase III Drosha and the RNA-binding protein DGCR8 (4, 5). There is evidence that the site of cleavage within the pri-miRNA is determined by the distance from the end of the hairpin containing the miRNA sequence (19). Processing is completed by Dicer after export of the pre-miRNA from the nucleus (20–23). Processing of miRNA precursors in plants is not yet understood in detail, but cleavage of the primary transcript to the mature miRNA duplex is thought to be carried out in the nucleus by DCL1. The RNA-binding protein HYL1 is necessary but may not be the only additional protein involved in processing. Mutations in the *SERRATE* (*SE*) gene have recently been reported to disrupt processing as well (24, 25).

Previous studies on miRNA precursor processing in *Arabidopsis* focused on analysis of miR163, for which a number of RNA species larger than the mature miRNA can readily be detected (26). Analysis of the primary transcripts and cleavage intermediates suggested that the pri-miR163 is cleaved in several steps to the mature miRNA (26). Mutations in the *DCL1* and *HYL1* genes were reported to result in aberrant cleavage of the precursors but did not result in significant accumulation of large precursors for miR163 (10, 26). In the present studies we found that neither full-length transcripts nor processing intermediates of the miR171a gene were sufficiently abundant to detect in wild-type plants, whereas several long transcripts in the 1.0- to 1.4-kb range accumulated in both *hyl1* and *dcl1* mutant plants. Careful analysis of the miR171a transcription unit identified at least three transcription start sites, of which the most frequently used is within the first intron of the gene, as defined by a previously reported transcription start site (27). Although we detected longer transcripts containing either part or all of the putative first exon, the most abundant transcript at the miR171a locus initiates at the pri-I site, 74 bp upstream from the base of the predicted stem–loop structure, and the transcripts that accumulate in *hyl1* and *dcl1* mutants appear to be partly or completely spliced transcripts originating at pri-I. Low levels of pre-miRNA could be detected by RT-PCR but were not sufficiently abundant to be detected by Northern blotting of total RNA in either the mutant or wild-type plants. Thus, the pri-miR171a precursor starts just upstream of the putative stem–loop structure containing the miRNA sequence, and miR171a is therefore not an intronic

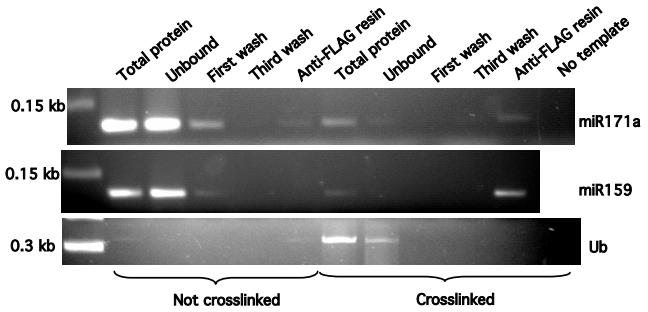

Fig. 5. Coimmunoprecipitation of miRNA precursors with HYL1. The HYL1 protein was immunoprecipitated from extracts of plants carrying a 35S:3×FLAG-HYL1–10×Myc construct after *in vivo* cross-linking with 1% formaldehyde (see *Materials and Methods*). RNA was isolated and amplified using primer pairs to detect both pre- and pri-miRNAs for miR171a and miR159a (see *SI Text* for primer sequences). Ubiquitin (Ub) mRNA was amplified as a measure of nonspecific binding. PCR amplification was for 35 cycles to detect the miRNA precursors and 25 cycles to detect the more abundant ubiquitin mRNA.

miRNA. Both HYL1 and DCL1 are required for the cleavage of the pri-miRNA. Pri-miRNA processing does not lead to significant accumulation of processed, polyadenylated transcripts in wild-type cells, indicating that processing is rapid and that the processing remnants are unstable.

Although both HYL1 and DCL1 are required for pri-miR171a processing, they have been identified in protein complexes of significantly different sizes. The HYL1 complex is ≈300 kDa (7), whereas DCL1 has been identified in a complex of >660 kDa (11). The observation that miRNA precursors coimmunoprecipitate with the HYL1 indicates that HYL1 is an integral component of the miRNA precursor-processing machinery. It has also been reported that HYL1 and DCL1 proteins interact directly (9). Although we can coimmunoprecipitate epitope-tagged recombinant HYL1 and DCL1 proteins, we have not detected fluorescence resonance energy transfer between HYL1-CFP and DCL1-YFP using either C- or N-terminal fusions of either protein, nor have we recovered DCL1 in the immunopurified HYL1 complex (L.S., M.-H.H., Z. Dong, and N.F., unpublished data). Nonetheless, we find that the two proteins colocalize and are often concentrated in nuclear bodies similar to Cajal bodies, which contain components of the siRNA silencing machinery, as well as many other RNA processing proteins (12, 16). The small, sometimes perinucleolar bodies in which HYL1 and DCL1 are concentrated are similar in size and location to Cajal bodies. However, they are distinguishable from Cajal bodies by the criterion that the *Arabidopsis* Atcoilin protein, a diagnostic Cajal body marker (18), does not colocalize with HYL1. The most straightforward interpretation of these observations is that the HYL1 and DCL1 complexes, although not tightly associated, function together in pri-miRNA processing in a distinct nuclear organelle. However, because we do not have direct evidence that the HYL1-bound miRNA precursors are in the HYL1/DCL1 bodies, an equally viable interpretation is that these nuclear bodies are assembly and storage sites for miRNA processing components, which then function in closer proximity to miRNA genes.

Materials and Methods

Plant Growth Conditions. *Arabidopsis hyl1-1*, *hyl1-2*, *hen1-1*, *hen1-4*, No-0, Col-0, and Ler plants were grown in soil at 23°C under short-day conditions for ≈4 weeks. Seeds of *dcl1-9* and *dcl1-7* mutant plants were germinated on MS plates (1× MS/0.8% agar/1% sucrose, pH 5.7) and grown under short-day conditions in a growth chamber for 10 days, then transferred to soil to grow for an additional ≈3 weeks.

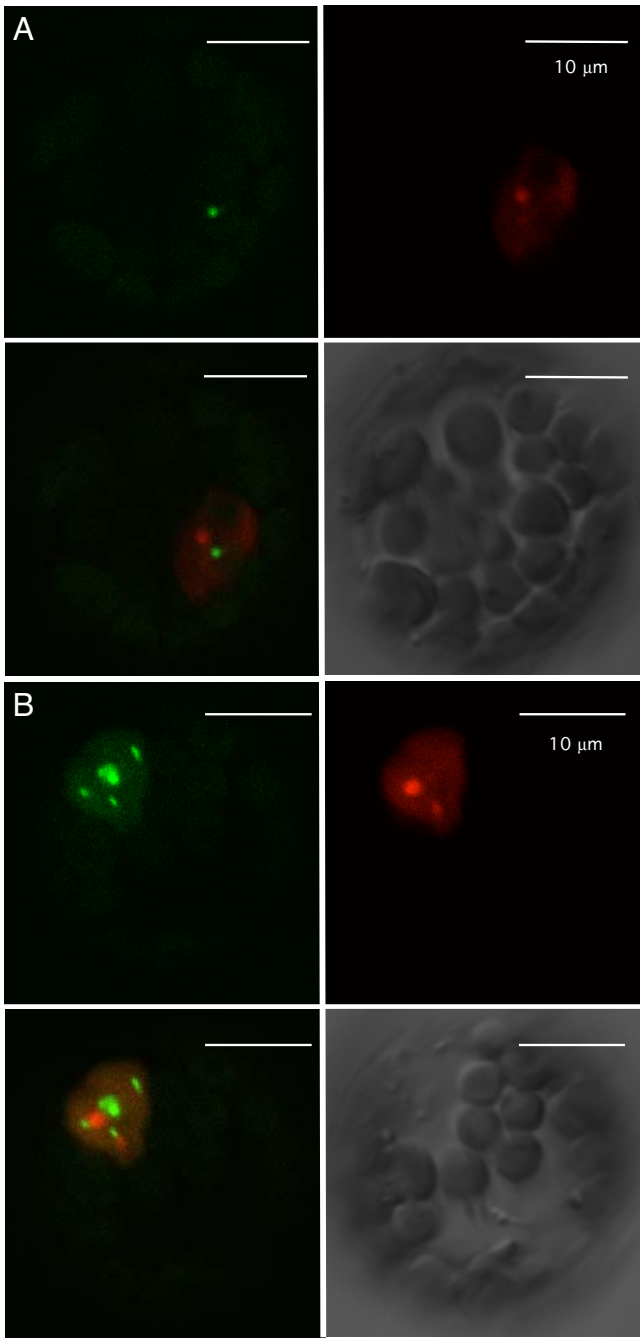

Fig. 6. HYL1 does not colocalize with the Cajal body marker Atcoilin. Protoplasts prepared from *Arabidopsis* leaves were transfected with plasmids carrying 35S-Atcoilin-GFP and 35S-HYL1-mCherry constructs. Shown are images of coilin (green, *A Upper Left* and *B Upper Left*), HYL1 (red, *A Upper Right* and *B Upper Right*), images of the superimposed coilin and HYL1 (*A Lower Left* and *B Lower Left*), and differential interference contrast microscopy images (*A Lower Right* and *B Lower Right*) for two cotransfected protoplasts.

RNA Isolation and Fractionation. Total RNA used in RNA fractionation and real-time RT-PCR experiments was isolated from the aerial parts of ≈4-week-old plants using the mirVana miRNA isolation kit (Ambion, Austin, TX). Total RNA for Northern blotting was isolated using TRIzol reagent (Invitrogen, Carlsbad, CA). Poly(A)$^+$ RNA was purified using the Oligotex mRNA mini Kit (Qiagen, Valencia, CA) from total RNA. Col-0 and *hyl1-2* total RNA were fractionated using Microcon YM-100 filters (Millipore) in the presence of 0.3 M NaOAc according to the manufacturer's

CELL BIOLOGY

instructions. Total RNA was centrifuged at 500 × *g* for 1 h at room temperature to separate RNA < 200 nt and RNA > 200 nt. Centrifugation was repeated at least once to remove most of the low-molecular-weight RNA.

RT-PCR and Real-Time PCR. RNA was treated with DNA-free DNase (Ambion) for 1 h at 37°C. cDNAs were generated using a High Capacity cDNA Archive Kit (Applied Biosystems, Foster City, CA) and random primers according to the manufacturer's instructions. Real-time PCR was performed using a QuantiTect SYBR Green PCR kit (Qiagen) in a 7300 Real-Time PCR system (Applied Biosystems). A "no amplification" control without reverse transcriptase and a "no template" control without added RNA template were incorporated to measure the level of DNA carryover from sample and reagents, and 18S rRNA was used as a loading control. The relative quantities of PCR products were calculated by the $\Delta\Delta C_T$ method as described in supporting information (SI) *Text*.

5′ and 3′ RACE. 5′ RACE was carried out on poly(A)$^+$ RNA using the GeneRacer kit (Invitrogen). The poly(A)$^+$ RNA was treated with calf intestinal phosphatase to remove phosphate groups from the 5′ ends of truncated molecules, after which the RNA was either treated (or not treated as a negative control) with tobacco acid pyrophosphatase to remove the 5′ caps from full-length molecules. An adapter was ligated to the 5′ ends, and the RNA was reverse-transcribed from an oligo(dT) primer using SuperScript III to generate cDNA. The cDNA was treated with RNaseH to remove the RNA strand, and the 5′ end of pri-171a was identified by nested PCR using two nested primers complementary to the 5′ adapter and two nested gene-specific primers (see *SI Text* for primer sequences).

Northern Blot Hybridization. Approximately 5 μg of poly(A)$^+$ RNA was fractionated on a 1.4% formaldehyde–agarose gel and transferred to Hybond N+ membrane (GE Healthcare, Piscataway, NJ). The primers used to amplify the intron 1 and exon probe fragments are given in *SI Text*. Probes were labeled by mixing RediPrimer II random priming labeling system (GE Healthcare) with ≈25 ng of template DNA and 5 μl of [α-^{32}P]dCTP and incubating at 37°C for 10 min. Free [α-^{32}P]dCTP was removed using Performa DTR gel filtration cartridges (Edge Biosystems, Gaithersburg, MD), and labeled probes were hybridized to poly(A)$^+$ RNA in PerfectHyb Plus hybridization buffer (Sigma–Aldrich, St. Louis, MO) at 68°C overnight. After hybridization and washing, the membranes were exposed to storage phosphor screen for 1–3 days and scanned using a Typhoon Scanner (GE Healthcare).

HYL1 Immunoprecipitation. Transgenic plants carrying a 35S:3×FLAG-HYL1–10×Myc construct were cross-linked *in vivo* with 1% formaldehyde in PBS (pH 7.4) by vacuum infiltration for 45 min at room temperature to fix protein–nucleic acid and protein–protein complexes (plants not subjected to cross-linking served as controls). The reaction was stopped with 125 mM glycine with gentle shaking for 10 min at room temperature. Proteins were isolated, and the HYL1 protein was immunoprecipitated using anti-FLAG resin. The immunoprecipitates were washed with 2 M urea and heated for 45 min at 70°C to reverse cross-linking. RNA was isolated using TRIzol reagent and amplified using primer pairs within the putative stem–loop structure of the precursor to detect both pri- and pre-miRNAs for miR171a and miR159a. Ubiquitin mRNA was amplified as a measure of nonspecific binding of RNA to the immunoprecipitated proteins.

Plasmids and Constructs. Plasmids containing HYL1 and DCL1 translational fusions with GFP, CFP, YFP, or mCherry were constructed as described in *SI Text*. SI Fig. 7 is a Western blot showing the expression of full-length DCL1 from the fusion construct in *Arabidopsis* protoplasts. Plasmids from which selected coding sequences were recloned were the kind gifts of the following investigators: pAVA321-YFP and pAVA321-CFP from Xuemei Chen (University of California, Riverside, CA), pBIN-GFP-AtCoilin from Peter Shaw (John Innes Centre, Colney, Norwich, U.K.), p4-GFP from Simon Gilroy (Pennsylvania State University), pGWB5 binary vector from Tsuyoshi Nakagawa (Shimane University, Shimane, Japan), and pRSET-B-mCherry from Roger Tsien (University of California at San Diego, La Jolla, CA).

Protoplast Isolation and Transfection. Protoplasts were isolated from leaves of 3- to 4-week-old Col-0 plants, and PEG-mediated transfection was carried out according to the protocol developed by J. Sheen (Harvard Medical School, Boston, MA). After transfection, protoplasts were incubated in the dark at room temperature for 16–20 h before observation.

Microscopy. GFP and YFP epifluorescence was observed using an Eclipse 90i microscope (Nikon, Melville, NY). GFP and YFP fluorescence was excited and collected through an Endow GFP HYQ BP filter cube (Ex 470/40, DM 525, BA 525/50). mCherry fluorescence was excited and collected through a G-2E/C*(TRITC) filter cube (EX540/25, DM 565, BA 605/55). Images were analyzed by using SIMPLEPCI software (version 6.1.1; Compix, Sewickley, PA). Confocal microscopy was done on an Olympus FV300 laser scanning confocal microscope (Olympus, Melville, NY). GFP was excited with the blue argon ion laser (488 nm), and emitted light was collected through a 510-nm long-pass filter and a 530-nm short-pass filter. mCherry was excited with a green HeNe laser (543 nm), and emitted light was collected through a 605-nm band-pass filter. Chloroplasts were excited with the blue argon laser (488 nm), and emitted light was collected through a 660-nm long-pass filter. Differential interference contrast microscopy images were collected simultaneously. Images were analyzed using Olympus FV300 software (version 4.0).

We thank Dr. Chris Malone for assistance with microscopy. This work was supported by National Science Foundation Grant IBN-0091650. J.L. was supported in part by Fulbright Junior Research Grant PPLJ/05/07.

1. Tomari Y, Zamore PD (2005) *Genes Dev* 19:517–529.
2. Henderson IR, Zhang X, Lu C, Johnson L, Meyers BC, Green PJ, Jacobsen SE (2006) *Nat Genet* 38:721–725.
3. Papp I, Mette MF, Aufsatz W, Daxinger L, Schauer SE, Ray A, van der Winden J, Matzke M, Matzke AJ (2003) *Plant Physiol* 132:1382–1390.
4. Denli AM, Tops BB, Plasterk RH, Ketting RF, Hannon GJ (2004) *Nature* 432:231–235.
5. Gregory RI, Yan KP, Amuthan G, Chendrimada T, Doratotaj B, Cooch N, Shiekhattar R (2004) *Nature* 432:235–240.
6. Lu C, Fedoroff N (2000) *Plant Cell* 12:2351–2366.
7. Han M-H, Goud S, Song L, Fedoroff N (2004) *Proc Natl Acad Sci USA* 101:1093–1098.
8. Vazquez F, Gasciolli V, Crete P, Vaucheret H (2004) *Curr Biol* 14:346–351.
9. Hiraguri A, Itoh R, Kondo N, Nomura Y, Aizawa D, Murai Y, Koiwa H, Seki M, Shinozaki K, Fukuhara T (2005) *Plant Mol Biol* 57:173–188.
10. Kurihara Y, Takashi Y, Watanabe Y (2006) *RNA* 12:206–212.
11. Qi Y, Denli AM, Hannon GJ (2005) *Mol Cell* 19:421–428.
12. Pontes O, Li CF, Nunes PC, Haag J, Ream T, Vitins A, Jacobsen SE, Pikaard CS (2006) *Cell* 126:79–92.
13. Yang Z, Ebright YW, Yu B, Chen X (2006) *Nucleic Acids Res* 34:667–675.
14. Wang XJ, Reyes JL, Chua NH, Gaasterland T (2004) *Genome Biol* 5:R65.
15. Cai X, Hagedorn CH, Cullen BR (2004) *RNA* 10:1957–1966.
16. Gall JG (2000) *Annu Rev Cell Dev Biol* 16:273–300.
17. Li CF, Pontes O, El-Shami M, Henderson IR, Bernatavichute YV, Chan SW, Lagrange T, Pikaard CS, Jacobsen SE (2006) *Cell* 126:93–106.
18. Collier S, Pendle A, Boudonck K, van Rij T, Dolan L, Shaw P (2006) *Mol Biol Cell* 17:2942–2951.
19. Han J, Lee Y, Yeom KH, Nam JW, Heo I, Rhee JK, Sohn SY, Cho Y, Zhang BT, Kim VN (2006) *Cell* 125:887–901.
20. Lee Y, Jeon K, Lee JT, Kim S, Kim VN (2002) *EMBO J* 21:4663–4670.
21. Lund E, Guttinger S, Calado A, Dahlberg JE, Kutay U (2004) *Science* 303:95–98.
22. Jiang F, Ye X, Liu X, Fincher L, McKearin D, Liu Q (2005) *Genes Dev* 19:1674–1679.
23. Gregory RI, Chendrimada TP, Cooch N, Shiekhattar R (2005) *Cell* 123:631–640.
24. Lobbes D, Rallapalli G, Schmidt DD, Martin C, Clarke J (2006) *EMBO Rep* 7:1052–1058.
25. Yang L, Liu Z, Lu F, Dong A, Huang H (2006) *Plant J* 47:841–850.
26. Kurihara Y, Watanabe Y (2004) *Proc Natl Acad Sci USA* 101:12753–12758.
27. Xie Z, Allen E, Fahlgren N, Calamar A, Givan SA, Carrington JC (2005) *Plant Physiol* 138:2145–2154.